Clusters of mobile molecules in supercooled water

Nicolas Giovambattista,[1,*] Sergey V. Buldyrev,[1,2] H. Eugene Stanley,[1] and Francis W. Starr[3]
[1]*Center for Polymer Studies and Department of Physics, Boston University, Boston, Massachusetts 02215, USA*
[2]*Department of Physics, Yeshiva University, 500 W. 185th St., New York, New York 10033, USA*
[3]*Department of Physics, Wesleyan University, Middletown, Connecticut 06459, USA*
(Received 21 April 2004; revised manuscript received 14 January 2005; published 13 July 2005)

[1]We study the spatially heterogeneous dynamics in water via molecular dynamics simulations using the extended simple point charge potential. We identify clusters formed by mobile molecules and study their properties. We find that these clusters grow in size and become more compact as temperature decreases. We analyze the probability density function of cluster size, and we study the cluster correlation length. We find that clusters appear to be characterized by a fractal dimension consistent with that of lattice animals. We relate the cluster size and correlation length to the configurational entropy, S_{conf}. We find that these quantities depend weakly on $1/S_{\mathrm{conf}}$. In particular, the linearity found between the cluster mass n^* and $1/S_{\mathrm{conf}}$ suggests that n^* may be interpreted as the mass of the cooperatively rearranging regions that form the basis of the Adam-Gibbs approach to the dynamics of supercooled liquids. We study the motion of molecules *within* a cluster, and find that each molecule preferentially follows a neighboring molecule in the same cluster. Based on this finding we hypothesize that stringlike cooperative motion may be a general mechanism for molecular rearrangement of complex, as well as simple liquids. By mapping each equilibrium configuration onto its corresponding local potential energy minimum or inherent structure (IS), we are able to compare the mobile molecule clusters in the equilibrium system with the molecules forming the clusters identified in the transitions between IS. We find that (i) mobile molecule clusters obtained by comparing different system configurations and (ii) clusters obtained by comparing the corresponding IS are completely different for short time scales, but are the same on the longer time scales of diffusive motion.

DOI: 10.1103/PhysRevE.72.011202 PACS number(s): 61.20.Gy, 61.25.Em, 64.70.Ja

I. INTRODUCTION

The dynamics of simple liquids well above the glass-transition temperature T_g are known to be spatially homogeneous, i.e., the mobility of the constituent atoms or molecules is distributed uniformly over space. As a liquid is cooled toward T_g the dynamics become spatially heterogeneous with transient regions of relative high and low mobility [1–3]. Both geometrical [4–8] and thermodynamic [9] explanations for the existence of spatially heterogeneous dynamics (SHD) in glass forming systems have been offered. The recent works of Garrahan and Chandler (GC) [4,5] use a geometric idea that particle mobility in a glass former is a result of facilitation (i.e., mobile particles assist their neighbors to become mobile), and that mobility propagation carries a direction [6,7]. The GC ideas are supported by a recent computer simulation on viscous silica [10].

In the SHD scenario, proposed by Adam and Gibbs (AG) [9], liquids relax through the motion of cooperatively rearranging regions (CRR) [11,12]. Furthermore, AG propose that SHD emerges as a consequence of lack of accessible states in configurational space [13]. Their predictions have been tested in experiments [14,15] and simulations [16,17], including the extended simple point charge (SPC/E) model [18,19] that we study. However, there are experimental results that seem to contradict the AG results (see, e.g. [20]). In this work, we interpret (in the context of the AG approach) the presence of the SHD in the SPC/E model of water.

In recent years, computer simulations [21–32] and experiments [33–38] have explored the concept of CRR and developed a more formal approach to identify local regions of enhanced or diminished mobility. In brief reports of some of the present results [39,40], molecular dynamics (MD) simulations found that heterogeneous dynamics of the SPC/E model for water [41] can be described by noncompact clusters of "mobile molecules," which we will call MM-clusters.

A key aspect of the AG approach is the concept of S_{conf}, the configurational part of the total entropy. AG proposed that S_{conf} could be related to both the average relaxation of the system and to the size of the CRR. However, AG did not provide a precise definition of S_{conf} for a liquid. Progress toward a more precise definition was made in 1969 by Goldstein [42], who considered the possible connection between the slowing down of liquid dynamics approaching T_g and the topography of the potential energy landscape (PEL). The PEL is the hypersurface defined by the potential energy as a function of the configurational degrees of freedom of the system [43,44]. The system at a given instant of time is represented by a point on the PEL determined by the coordinates of all the molecules. The dynamics of the system can be described by the motion of the system point on the PEL. At sufficiently high temperatures, the system can freely explore the entire PEL. As temperature is lowered toward T_g, the accessible portion of the PEL becomes more limited. At sufficiently low temperatures, the motion of the system can be described by oscillations around PEL local minima and transitions between one local minimum and another. A con-

*Present address: Department of Chemical Engineering, Princeton University, Princeton, NJ 08544–5263.

figuration in real space corresponding to a PEL local minimum is called an inherent structure (IS). Stillinger [43] formalized the concept of S_{conf} by mathematically relating it to the number of minima accessible to the system at equilibrium.

The evolution of the system in real space can be related to the transitions between the PEL minima. Similar to the MM-clusters observed in the evolution of the equilibrium system, the infrequent transitions between IS at low T involve the rearrangement of few molecules which also form clusters [45,46]. We call these clusters "IS-transition clusters" (IST-clusters). A natural question that arises is what, if any, is the relationship between MM-clusters and IST-clusters, and can these clusters be related to S_{conf}, as proposed by AG.

The MM-clusters have been studied extensively in Lennard-Jones (LJ) and polymer systems.[21–32] Here we consider if the MM-clusters observed in those systems are different from the MM-clusters observed in supercooled water which has a predominantly tetrahedral structure. This work is organized as follows. In the next section we give details of our molecular dynamics simulations. In Sec. III we describe how we identify the MM-clusters. The dependence of the cluster properties on temperature is reported in Sec. IV, and the motion of the mobile molecules within a cluster is discussed in Sec. V. In Sec. VI we study the relation between the MM-clusters and the IST-clusters [46]. In Sec. VII we summarize the results and compare with earlier works on atomic and polymer systems [21–32].

II. SIMULATIONS

We perform MD simulations of the SPC/E model [41] of water for a system of 1728 molecules, at a fixed density $\rho = 1\ \mathrm{g/cm^3}$. We simulate temperatures ranging from 200 to 260 K at 10 K intervals. For each state point, we run two independent trajectories to improve statistics. The details of the numerical procedure can be found in Ref. [47]. We measure the mean-square displacement (MSD) for times long enough so molecules are able to move at least two molecular diameters. In this way, a clear diffusive regime can be observed from the MSD for long times. We obtain the values of the diffusion coefficient from the slope of the MSD for long times and find that our values are consistent to those reported in Ref. [47]. In accord with the mode coupling theory [48], we find that for the SPC/E model the diffusion coefficient D decreases with T as

$$D \sim (T - T_{MCT})^{\gamma}, \tag{1}$$

where $\gamma = 2.8$ and the mode coupling temperature $T_{MCT} \approx 194$ K [47].

To study the IST-clusters, we must perform many energy minimizations to generate the IS configurations. Because the conjugate gradient minimization algorithm used to generate the IS is computationally expensive, it becomes prohibitive to do many minimizations with large systems. Hence, to compare the MM-clusters with the IST-clusters, we also simulated a 216 molecule system at $T = 210$ K and $\rho = 1\ \mathrm{g/cm^3}$. These results are also averaged over two independent simulations of more than 60 ns each, i.e., more than 10 times the α-relaxation time at this temperature [47].

III. DEFINITION OF MOBILE MOLECULE CLUSTERS

To compare the MM-clusters of the SPC/E model of water with the MM clusters of binary LJ systems, polymer systems, and colloids, we use the same approach used in Refs. [23,30,33,38]. Specifically, we calculate the self-part of the time-dependent van Hove correlation function [49]

$$G_s(r,t) \equiv \frac{1}{N}\sum_{i=1}^{N} \langle \delta[|\vec{r}_i(t) - \vec{r}_i(0)| - r]\rangle, \tag{2}$$

where $\langle \cdots \rangle$ represents average over independent runs and possible starting configurations and $\vec{r}_i(t)$ are the coordinates of the oxygen atom of the ith molecule. The probability density of finding an oxygen atom at time t and at distance r from its initial position at $t=0$ is $4\pi r^2 G_s(r,t)$.

At both short time intervals (when molecules move ballistically) and long time intervals (when the molecular motion can be described as a diffusive process) $G_s(r,t)$ can be fit by a Gaussian approximation,

$$G_0(r,t) = \left[\frac{3}{2\pi\langle r^2(t)\rangle}\right]^{3/2} \exp[-3r^2/2\langle r^2(t)\rangle], \tag{3}$$

where $\langle r^2(t)\rangle$ is the mean-square displacement of the oxygen atoms. Deviations of $G_s(r,t)$ from $G_0(r,t)$ are known to be pronounced at intervals between the ballistic and diffusive motion, i.e., at times corresponding to the vibration of the molecules within the cage formed by neighbor molecules. The deviation of $G_s(r,t)$ from $G_0(r,t)$ can be quantified by a "non-Gaussian parameter" [50],

$$\alpha_2(t) \equiv \frac{3}{5}\langle r^4(t)\rangle / \langle r^2(t)\rangle^2 - 1. \tag{4}$$

The larger $\alpha_2(t)$ is, the larger the deviations of $G_s(r,t)$ from $G_0(r,t)$. As indicated in Fig. 1(a), we define t^* as the value of time at which $\alpha_2(t)$ is maximum.

As indicated in Fig. 1(b), we define r^* as the largest value of r at which $G_s(r,t^*)$ and $G_0(r,t^*)$ intersect. Similar to simple liquids $G_s(r,t^*)$ has a tail for $r > r^*$ where $G_s(r,t^*) > G_0(r,t^*)$. In other words, there is an excess of molecules that have moved a distance $r > r^*$, when compared with the expectations of a Gaussian distribution. We find that r^* is in the range 0.20–0.25 nm for all T, slightly smaller than the typical nearest-neighbor separation [51]. The fraction of molecules that have moved a distance $r > r^*$ at $t = t^*$ is given by

$$\phi \equiv \int_{r^*}^{\infty} 4\pi r^2 G_s(r,t^*) dr. \tag{5}$$

Depending on T, we find $0.06 < \phi < 0.08$. Since ϕ varies weakly with temperature, we fix $\phi = 0.07$ for all T to simplify our analysis. Similar values of ϕ were found in simulations of atomic systems in Refs. [22,23] and polymer melts [30], as well as in experiments on colloidal systems [38]. Following [23], we define the mobility of the ith molecule at a given time t_0 as the maximum displacement of the oxygen atom in the interval $[t_0, t_0 + \Delta t]$, i.e.,

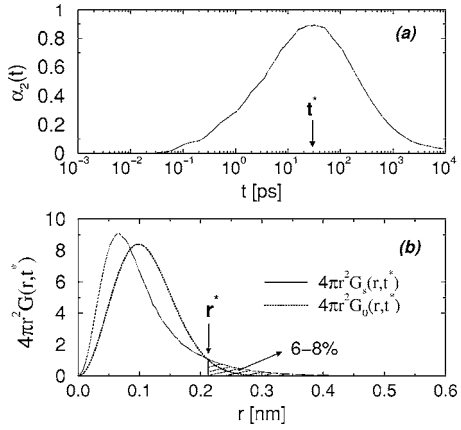

FIG. 1. (a) Definition of t^*, the time at which the maximum of the non-Gaussian parameter $\alpha_2(t)$ occurs (example at $T=220$ K). (b) Definition of the distance r^* as the intersection of the van Hove correlation function $G_s(r,t^*)$ and its Gaussian approximation $G_0(r,t^*)$ obtained using $\langle r^2(t^*)\rangle$, for $T=220$ K. The tails of the distributions cross at $r^* \approx 0.225$ for all temperatures. This paper focuses on the subset of mobile molecules that correspond to displacements larger than r^* over a time interval t^*. These molecules represent a fraction, 0.06–0.08, of the system [shaded area in panel (b)].

$$\mu_i(t_0,\Delta t) = \max\{|\vec{r}_i(t_0) - \vec{r}_i(t+t_0)|, t_0 \leqslant t \leqslant t_0 + \Delta t\}. \quad (6)$$

We will be interested in the "mobile molecules" defined as the fraction ϕ of molecules with largest μ_i. We define a MM-cluster at time t_0 over an observation time Δt as those mobile molecules whose nearest-neighbor oxygen-oxygen distance at time t_0 is less than 0.315 nm, the first minimum of the oxygen-oxygen radial distribution function $g_{OO}(r)$ [52].

MM-clusters can become quite large. Hence to avoid strong finite size effects that can result from the spanning of clusters across the system, we must ensure that our system is large enough that the probability of finding a spanning cluster $P_{\text{span}}(\phi)$ is small. Figure 2 shows $P_{\text{span}}(\phi)$ as a function of the fraction ϕ of mobile molecules at $T=200$ K (the lowest temperature studied where correlations are expected to be greatest). We find that $P_{\text{span}}(\phi)$ becomes nonzero around $\phi \approx 0.1$ and reaches 0.5 at $\phi \approx 0.18$. Since MM-clusters have a smaller size at higher T, our system size is large enough that for $\phi=0.07$ no spanning MM-clusters should be present at any T studied. For comparison we include in Fig. 2 the spanning probability obtained for clusters formed by choosing random molecules. The difference between the two curves reflects the cooperativity associated with the MM-clusters. Similar results have also been found for polymeric systems [30].

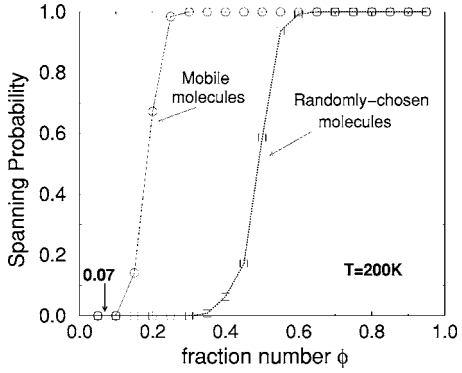

FIG. 2. Probability density function to find a spanning MM-cluster as a function of the fraction ϕ of mobile molecules composing the cluster. We choose the simulated T at which the clusters are largest, i.e., $T=200$ K. We also include the corresponding spanning probability for clusters formed by randomly chosen molecules. The percolation threshold p_c (where the spanning probability is 0.5) is ≈ 0.18 for MM-clusters and ≈ 0.49 for clusters formed by randomly chosen molecules. Note that there are no spanning MM-clusters at $\phi=0.07$.

$$\langle n(\Delta t)\rangle_w \equiv \frac{\sum n^2 P(n,\Delta t)}{\sum n P(n,\Delta t)} = \frac{\langle n^2(\Delta t)\rangle}{\langle n(\Delta t)\rangle}, \quad (7)$$

where $P(n,\Delta t)$ is the probability of finding clusters of size n within an observation time Δt. $\langle n(\Delta t)\rangle_w$ measures the average size of a MM-cluster to which a randomly chosen molecule belongs. Percolation theory [53] predicts that clusters formed by randomly chosen molecules have a nontrivial dependence of the cluster size on the fraction of chosen molecules ϕ. Therefore, to quantify how cooperativity affects the MM-cluster size and eliminate effects due to clusters formed by randomly chosen molecules, we use a normalized quantity, $\langle n(\Delta t)\rangle_w / \langle n_r\rangle_w$, where $\langle n_r\rangle_w$ is the weight average cluster mass when choosing randomly $N\phi$ molecules. This removes any random contribution from $\langle n(\Delta t)\rangle_w$, such that

$$\langle n(\Delta t)\rangle_w / \langle n_r\rangle_w = 1 \quad (8)$$

means that the clusters are the same size as those that would be formed by a random process.

The dependence of $\langle n(\Delta t)\rangle_w / \langle n_r\rangle_w$ on the observation time Δt for different T was studied in a preliminary work [39]. Figure 3(c) in Ref. [39] shows that at high temperature ($T \gtrsim 240$ K), there is a weak T-independent maximum at $t \approx 1$ ps reflecting correlations in vibrational motion due to hydrogen bonds. At lower $T \lesssim 240$ K, $\langle n(\Delta t)\rangle_w / \langle n_r\rangle_w$ develops a T-dependent maximum at $\Delta t = t_{\max}(T)$ that shifts to larger times as T decreases. For all T studied, it is found that t^* is slightly larger than $t_{\max}$ [39]. It has been shown that t^* indicates the time scale corresponding to the escape of the molecules from the cages formed by the neighboring molecules, at the beginning of the "diffusive regime" [39]. The fact that t^* and $t_{\max}$ have similar values implies that MM-clusters reach their maximum size for an observation time Δt approximately corresponding to the time at which molecules leave their cages. In this section, we focus on the T depen-

IV. DEPENDENCE OF MM-CLUSTER PROPERTIES ON TEMPERATURE

A. Cluster mass: Number of participating molecules

The size of MM-clusters can be quantified using the weight average cluster mass

TABLE I. Fitting parameters for $P(n,T) \sim n^{-\tau} e^{-n/n_0}$, where $\tau = \tau(T)$ and $n_0 = n_0(T)$.

T	τ	n_0
200	2.17	33.4
210	1.99	7.4
220	2.09	8.0
230	1.96	4.3
240	2.04	4.9
250	2.01	4.0
260	1.96	3.6

dence of the MM-clusters obtained at $\Delta t = t^*$. Our conclusions are unaffected if we chose $\Delta t = t_{\max}$ instead of $\Delta t = t^*$.

The properties of the MM-clusters can also be examined in terms of the properties of clusters defined in percolation theory, for example, by studying the probability density function $P(n,T)$ of finding a MM-cluster with n molecules at a given T. $P(n,T)$ is shown in a previous work [40] for different T and for a fraction $\phi = 0.07$ of mobile molecules. The distributions can be fitted with the *Ansatz* used in percolation theory [53],

$$P(n,T) \sim n^{-\tau} e^{-n/n_0}, \tag{9}$$

where $n_0 = n_0(T)$ is a characteristic cluster size at T and the exponent $\tau = \tau(T)$ may depend also on T. The functional form of $P(n,T)$ does not depend on ϕ, although changing ϕ changes the values of $n_0(T)$ and $\tau(T)$. The values of $\tau(T)$ and $n_0(T)$ obtained for $\phi = 0.07$ are tabulated in Table I. We are unable to obtain highly accurate estimates of $n_0(T)$, but we do find a trend that $n_0(T)$ increases with decreasing T, consistent with clusters becoming progressively larger upon cooling. From Table I, we see that $\tau(T) = 2.1 \pm 0.1$ for all T. This value is consistent with the values

$$\tau(T) \approx 1.9 \tag{10a}$$

for LJ particles [23] and

$$\tau(T) = 2.2 \pm 0.2, \tag{10b}$$

for colloidal suspensions [38]. Thus τ may be independent of the details of the potential. A similar expression for $P(n,T)$ was also found in [30] for a polymer melt but with a smaller exponent

$$\tau(T) = 1.62 \pm 0.12. \tag{10c}$$

This smaller value may be due to the constraints in the motion of the monomers, which are bonded to neighboring monomers in the same polymer. Note that the value of the exponent τ found for MM-clusters is very close to the value predicted for the distribution of three-dimensional percolation clusters $\tau_{perc} = 2.19$, which is satisfied by the clusters of randomly selected molecules at the percolation threshold. As shown in Fig. 2, the random percolation threshold for our system is ≈ 0.5, much larger than the fraction of mobile molecules $\phi = 0.07$. Thus the observed exponent τ for MM-clusters is not a consequence of percolation theory [53].

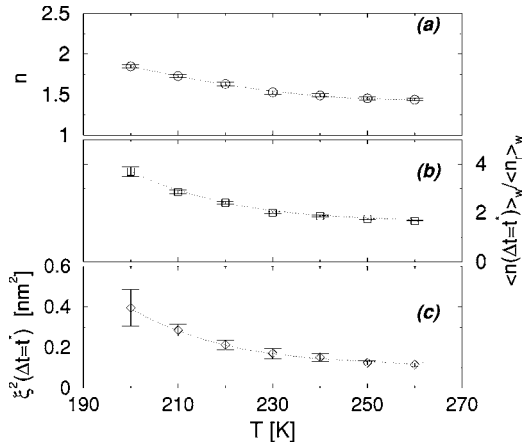

FIG. 3. Demonstration that three critical quantities increase nonlinearly as T decreases: (a) the non-normalized average number of molecules $n^* \equiv \langle n(\Delta t = t^*) \rangle$, (b) the normalized weight cluster mass $\langle n(\Delta t = t^*) \rangle_w / \langle n_r \rangle_w$, and (c) the correlation length $\xi(\Delta t = t^*)$. Dotted lines are a guide to the eye.

Figure 3(a) shows the T-dependence of average maximum number of molecules in a MM–cluster for $n^* \equiv \langle n(\Delta t = t^*) \rangle$ (without normalization), and Fig. 3(b) shows the normalized weight average cluster mass $\langle n(\Delta t = t^*) \rangle_w / \langle n_r \rangle_w$. Both quantities measure a characteristic cluster size in terms of the number of molecules, and they appear to increase nonlinearly with decreasing T. However, we cannot reliably predict the functional form of this T dependence, or how strongly the cluster size may grow at T below 200 K, the lowest T we simulate.

B. Cluster size: Spatial dimensions

We next aim to better characterize the morphology of the clusters by estimating the geometric size. We first must obtain a characteristic spatial dimension of the MM-cluster size, which we evaluate using the correlation length [Fig. 3(c)]

$$\xi^2 \equiv \frac{\sum_r r^2 g(r)}{\sum_r g(r)}, \tag{11}$$

where $g(r)$ is the correlation function or pair connectivity [53] defined as the probability that two molecules belonging to the same MM-cluster are separated by a distance r. Here, ξ can be interpreted as the root-mean-square distance between two molecules in a cluster [53]. For a given observation time Δt, $\xi(\Delta t)$ can be rewritten in terms of the radius of gyration $R_g(n)$ [53],

$$\xi^2(\Delta t) = \frac{2 \sum R_g(n)^2 n^2 P(n, \Delta t)}{\sum n^2 P(n, \Delta t)}, \tag{12}$$

where

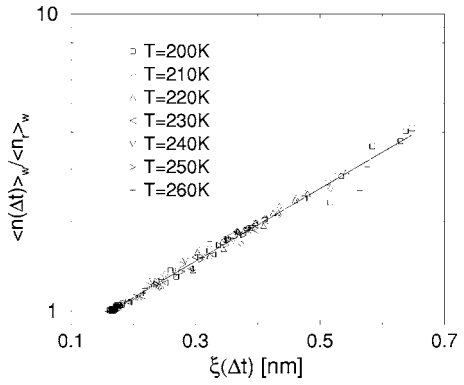

FIG. 4. Log-linear plot of the weight averaged cluster mass $\langle n(\Delta t)\rangle_w/\langle n_r\rangle_w$ as a function of the correlation length $\xi(\Delta t)$. We show points for all temperatures and observation times Δt. An exponential dependence of $\langle n(\Delta t)\rangle_w/\langle n_r\rangle_w$ with $\xi(\Delta t)$ has been also found in a polymer melt [30].

$$R_g^2(n) \equiv \frac{\sum_{i,j} |\vec{r}_i - \vec{r}_j|^2}{2n^2}. \tag{13}$$

Here $\vec{r}_i$ and $\vec{r}_j$ are the positions of oxygen atoms of molecules i and j within the same cluster. The dependence of $\xi(\Delta t)$ with the observation time is similar to the behavior of $\langle n(\Delta t)\rangle_w/\langle n_r\rangle_w$. Furthermore, from Fig. 3(c) we observe that $\xi^2(\Delta t=t^*)$ increases monotonically with decreasing T, and for $T=200$ K we find $\xi^2(\Delta t=t^*)\approx 0.4$ nm^2. This indicates a typical cluster size of $\xi\approx 0.63$ nm at $T=200\ \mathrm{K}\approx 1.03\ \mathrm{T_{MCT}}$.

While we cannot accurately estimate ξ at near T_g—significantly below the lowest $T=200$ K that we can access in simulations—we can extrapolate values consistent with experimental estimates of the cluster size. Using *o*-terphenyl [54] as an example, the size sensitivity of the probe molecules to heterogeneous dynamics indicates a typical cluster size of ≈ 2.5 nm at the glass transition. The cluster size in a LJ system [21] was also estimated to be of the order of 1 nm at $T\approx 1.04\ T_{MCT}$. Future simulations should focus on the cluster size at lower T to confirm that clusters found in simulations have a comparable size to those found experimentally.

The similar behavior of $\langle n(t^*)\rangle_w/\langle n_r\rangle_w$, n^*, and $\xi(t^*)$ upon cooling in Fig. 3 suggests that these quantities are related. In Fig. 4 we show $\langle n(\Delta t)\rangle_w/\langle n_r\rangle_w$ versus $\xi(\Delta t)$ and find an exponential dependence

$$\frac{\langle n(\Delta t)\rangle_w}{\langle n_r\rangle_w} \sim e^{\xi(\Delta t)/\ell}, \tag{14}$$

where $\ell=0.35$ nm. Exponential dependence of $\langle n(\Delta t)\rangle_w/\langle n_r\rangle_w$ with $\xi(\Delta t)$ was also observed in polymer melts [30], but an explanation of this behavior has been elusive. In the following we give a plausible argument explaining how such exponential dependence can arise from the branching structure of the clusters.

If one assumes that the MM-clusters have a branching treelike structure in which each molecule has on average $q \leqslant 4$ neighbors (the typical coordination number of a bulk water molecule is 4), then the mass of the cluster with a radius $R\approx j\ell_0$ (where $\ell_0=0.28$ nm is the average oxygen-oxygen nearest-neighbor distance, and $j=1,2,\ldots$ is an integer) grows as

$$\frac{\langle n(\Delta t)\rangle_w}{\langle n_r\rangle_w} \sim (q-1)^j. \tag{15}$$

Substituting $j=R/\ell_0$ into Eq. (15) we get

$$\frac{\langle n(\Delta t)\rangle_w}{\langle n_r\rangle_w} \approx e^{(R/\ell_0)\ln(q-1)}. \tag{16}$$

Thus if we identify $R=\xi$ then from Eq. (14) it follows that $\ell=\ell_0/\ln(q-1)$. Using the value $\ell=0.35$ nm, this suggests $q=3.2$, i.e., an average of 3.2 neighbors for each molecule, consistent with the expectation that $q\leqslant 4$. We calculate q at $T=200$ K and $\Delta t=t^*$, and find that $q\approx 2.65$ for large clusters, smaller than the estimated value of 3.2. Therefore, the approximation Eq. (16) may serve as a first step to rationalize the relationship given by Eq. (14), but a more detailed model is needed.

We can expect from Eq. (14) that the number of molecules n in a MM-cluster and the average radius of gyration $R_g(n)$ are also related by an exponential function,

$$n \sim e^{bR_g(n)}, \tag{17}$$

where b is a constant. On the other hand, large clusters cannot obey this formula due to the constraint $n\leqslant c[R_g(n)]^3$ where c is a constant proportional to the number density of molecules. Moreover, percolation theory [53] predicts that at percolation threshold, clusters are fractal objects with

$$n \sim [R_g(n)]^{d_f}, \tag{18}$$

where $d_f=2.52$ in three dimensions. Below the percolation threshold, large clusters are expected to behave as lattice animals [53] with smaller fractal dimension, $d_f=2$ in three-dimensions. Lattice animals [55] are connected clusters of n particles counted with equal statistical weight. The clusters in percolation theory are counted with weight $(1-\phi)^t$, where t is the cluster perimeter. Thus elongated percolation clusters with large perimeters are taken with smaller weight than compact clusters with small perimeters. Consequently the fractal dimension of percolation clusters is larger than that of lattice animals. For very small ϕ, the fractal dimension of large clusters must coincide with the fractal dimension of lattice animals. These ideas were put forward by Bouchaud [56] for dynamics of granular media and in Ref. [57] for glassy dynamics. They suggested that the regions of fast dynamics are delimited by the contour lines of a random field. Thus Bouchaud conjectured that dynamic heterogeneities may be lattice animals of fractal dimension $d_f=2$ in three dimensions (and $d_f=1.56$ in two dimensions).

In order to test the predictions that small clusters will obey Eq. (17), while large clusters will be lattice animals, we plot the values of n versus $R_g(n)$ in semilogarithmic and double-logarithmic scales for $T=200$ K [Figs. 5(a) and 5(b)]. One can clearly see that as predicted, the slope of the graph on the semilogarithmic plot decreases with $R_g(n)$, while on the double-logarithmic plot it increases, approaching the

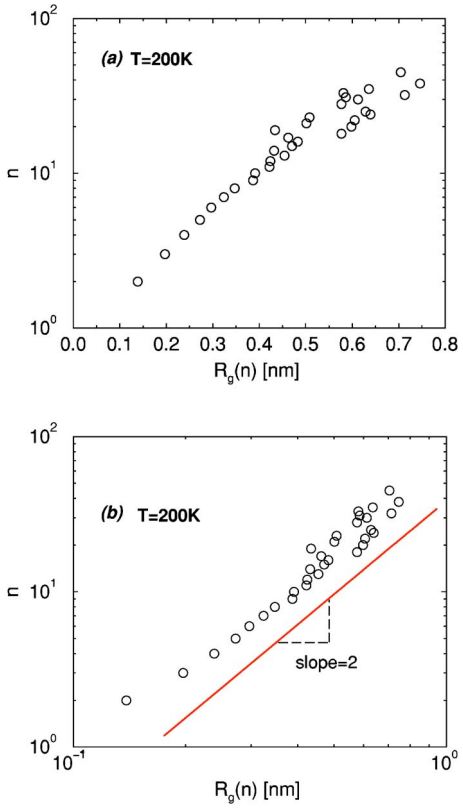

FIG. 5. (Color online) Average cluster size n as a function of the radius of gyration $R_g(n)$ for MM-clusters defined at $\Delta t=t^*$ and $T=200$ K. We show the data in both (a) semilog and (b) log-log scale. The exponential dependence only appears valid for small n. On the double-logarithmic plot the slope increases consistent with an asymptotic limit $d_f=2$ (where d_f is the fractal dimension of the MM-clusters). Since for lattice animals in three dimensions $d_f=2$, the value of the slope found in (b) suggests that the MM-clusters resemble lattice animals.

asymptotic limit $d_f=2$. Hence these clusters may be lattice animals. The value $d_f=2$ is also in agreement with the determination of Weeks *et al.* for dense, three-dimensional colloidal glasses [38].

C. Relation between MM-clusters and cooperatively rearranging regions

The developing study of SHD follows from the seminal work of AG, who discussed the relaxation of liquids in terms of local cooperatively rearranging regions (CRR). In this section we discuss the possible relations between the approach of AG and the phenomenology of the MM-clusters. AG predict that the configurational entropy S_{conf} and the diffusion constant D are related by

$$D \approx \exp\left(\frac{-A}{TS_{\text{conf}}}\right). \tag{19}$$

Although in some cases this expression could not be confirmed [20], it was successfully tested for the SPC/E model [18,19,58] and other liquids [16,17]. AG also predict that the size z of a CRR is related to S_{conf} via

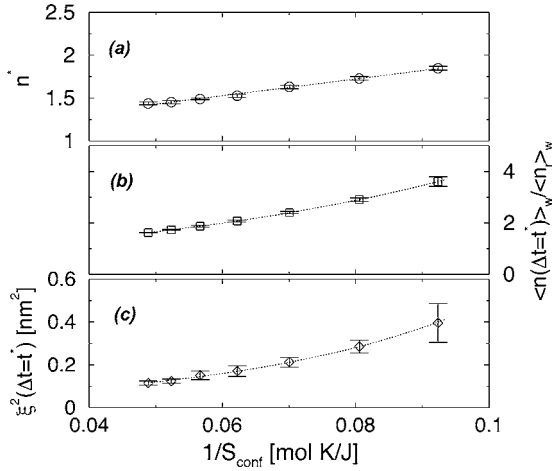

FIG. 6. Dependence on $1/S_{\text{conf}}$ of (a) the non-normalized average cluster mass $n^* \equiv \langle n(\Delta t=t^*)\rangle$, (b) the normalized weight averaged cluster mass $\langle n(\Delta t=t^*)\rangle_w/\langle n_r\rangle_w$, and (c) the correlation length $\xi(\Delta t=t^*)$. The three quantities are weak dependent on $1/S_{\text{conf}}$ and only n^* can be satisfactorily fit by a straight line (see dotted lines).

$$z = \frac{Ns_{\text{conf}}(z)}{S_{\text{conf}}}, \tag{20}$$

where $s_{\text{conf}}(z)$ is the configurational entropy associated to a CRR of size z, and S_{conf} is the total configurational entropy of the system. Assuming that the T-dependence of $s_{\text{conf}}(z)$ is weak in comparison to that of S_{conf}, as can be expected since $z \ll N$ and the configurational entropy is an extensive property, then Eq. (20) reduces to

$$z \propto \frac{1}{S_{\text{conf}}}. \tag{21}$$

Given the conceptual overlap between CRR described by AG and the MM-clusters we study, it is natural to ask if the MM-clusters can be identified with the CRR. To this end, we plot $\langle n(\Delta t=t^*)\rangle_w/\langle n_r\rangle_w$, n^*, and $\xi(\Delta t=t^*)$ as functions of $1/S_{\text{conf}}$ (Fig. 6). All three quantities have weak dependences on $1/S_{\text{conf}}$ for large S_{conf}. The finding that

$$(n^* - 1) \propto \frac{1}{S_{\text{conf}}} \tag{22}$$

has an important consequence. We can recover the AG prediction, Eq. (21), if we identify $z \approx n^* - 1$, and hence the MM-clusters may be said to describe the CRR of the AG approach. This finding thus suggests a quantitative connection between the SHD approach and the AG approach.

As discussed previously in Ref. [39], by combining Eqs. (19) and (22) one obtains

$$\frac{n^* - 1}{T} \propto -\log D. \tag{23}$$

This equation relates the size of the MM-clusters with the diffusion coefficient. From this expression, we can estimate the value of n^* at T_g and compare it with experimental values. To do this, first we evaluate Eq. (23) at T_g and at T_{MCT}, and then we form the ratio of both expressions,

$$\frac{n^*(T_g)-1}{T_g}\frac{T_{MCT}}{n^*(T_{MCT})-1}=\frac{\log D(T_g)}{\log D(T_{MCT})}. \quad (24)$$

In accord with Ref. [47], we find that for the SPC/E model $T_{MCT}=194$ K. Thus we approximate $D(T_{MCT}=194\ \mathrm{K})$ by $D(200\ \mathrm{K})$ and use the value obtained from our simulations $D(200\ \mathrm{K})\approx 10^{-8}\ \mathrm{cm}^2/\mathrm{s}$ [47]. Therefore we obtain $D(T_{MCT}=194\ \mathrm{K})\approx 10^{-8}\ \mathrm{cm}^2/\mathrm{s}$. On the other hand, typical values of D at T_g are 10 or more orders of magnitude smaller than those of normal liquids [59]. Thus, assuming $D(T_{MCT})\approx 10^{10}D(T_g)$, Eq. (24) reduces to

$$\frac{n^*(T_g)-1}{T_g}\frac{T_{MCT}}{n^*(T_{MCT})-1}\approx\frac{-18}{-8}=2.25. \quad (25)$$

We approximate $n^*(T_{MCT})$ by $n^*(200\ \mathrm{K})$ and use the value we obtain from our simulations, $n^*(200\ \mathrm{K})=1.86$. We also assume $T_{MCT}/T_g\approx 1.3$, as it is commonly found in glass-forming liquids. Therefore, replacing $n^*(T_{MCT})\approx 1.86$ and $T_{MCT}/T_g\approx 1.3$ in Eq. (25), we get $n^*(T_g)\approx 2.5$. This value for $n^*(T_g)$ corresponds to a linear size of 0.6–0.9 nm, in accord with estimates from calorimetric data made for different glass-forming liquids [60] which give radii for SHD at T_g in the range 0.7–2.2 nm. Moreover, Ref. [36] finds that SHD in o-terphenyl (OTP) extends to length scales of 2.5 nm at T_g. The size of the OTP molecule is $\approx$1 nm, so our estimate for $n^*(T_g)$ is also consistent with [36].

For the Dzugutov potential, it was found that $n^*\propto 1/S_{\mathrm{conf}}$, and not $(n^*-1)\propto 1/S_{\mathrm{conf}}$. As discussed in Ref. [61], the first expression was proposed based on the AG relation which was suggested for temperatures near T_g. At moderately high T, cooperativity is no longer important for particle motion, and so we expect n^* approaches the value for randomly chosen molecules (close to one), while $1/S_{\mathrm{conf}}$ is still larger than zero (the limit $1/S_{\mathrm{conf}}\to 0$ corresponds to the limit $T\to\infty$, i.e., to the very high T limit). As a result, an extrapolation of n^* to the $1/S_{\mathrm{conf}}=0$ limit will result in a nonzero value of n^*. The exact value of the extrapolated n^* will be system dependent, as the $1/S_{\mathrm{conf}}$ axis will be system dependent, as the temperature where cooperativity becomes unimportant is system dependent. Hence, in Ref. [39], we fit data for n^* as a function of $1/S_{\mathrm{conf}}$ and found a linear relationship

$$(n^*-a)\propto\frac{1}{S_{\mathrm{conf}}}, \quad (26)$$

where a is a constant. We select $a=1$, so that $(n^*-a)\to 0$ for $T\to\infty$, for which $1/S_{\mathrm{conf}}\to 0$. However, Eq. (21) is expected to hold only for low T. Therefore there are no physical requirements that support $a=1$, and one can only suggest that $(n^*-a)\propto 1/S_{\mathrm{conf}}$ (where a is system dependent). With this revised interpretation, the CRR of Adam and Gibbs may be related with the MM-clusters in both the SPC/E and the Dzugutov potential simulations.

We also note that in a recent MD simulation of silica (a "strong" liquid) where simulations were performed above and below T_{MCT} (i.e., in a wider range of T than in the present work and in [61]) a weak but nonlinear dependence of (n^*-1) with $1/S_{\mathrm{conf}}$ [62] was found. It is not clear whether Eq. (26) holds for silica (for $a\neq 1$), but the case of silica suggests that Eq. (26) is an approximation that may not be generalized to all liquids. Note that we can test Eq. (26) only in a relatively narrow range of temperatures, $200\ \mathrm{K}\leqslant T\leqslant 260$ K. In this T range, $1/S_{\mathrm{conf}}$ changes by less than a factor of 2. Thus small deviations from linearity may not be well seen. In a wider T range the predictions of the AG approach may not hold. However, the AG theory provides a simple conceptual framework to understand the dynamics of supercooled liquids in terms of SHD.

V. CORRELATED MOTION OF MOLECULES WITHIN MM-CLUSTERS

For LJ and polymer systems [23,31], it has been found that the MM clusters consist of one or more "strings"—groups of particles that follow each other in a roughly linear fashion. In this section, we focus on the correlations among the displacements of the molecules within MM-clusters to determine if a similar behavior exists in the MM-clusters of water, as well as to explore what role, if any, hydrogen bonds play in determining motion within the cluster. We will determine if molecules move in a stringlike fashion by checking (i) if displacements of neighboring oxygen atoms are parallel, (ii) if the magnitude of the displacements of neighboring oxygen atoms are comparable, and finally (iii) if these displacements are approximately collinear with the vector connecting both oxygens.

First, for each MM-cluster, we identify all pairs of nearest-neighbor molecules, i.e., those molecules in a cluster with an oxygen-oxygen distance less than 0.315 nm. We focus on the angle θ between the "maximum displacement vectors" $\vec{\mu}_{O1}(\Delta t)$ and $\vec{\mu}_{O2}(\Delta t)$ of pairs of neighboring oxygen atoms O_1 and O_2 in the same MM-cluster, during an observation time Δt. To determine if the displacements of neighboring molecules are parallel, we plot the probability density function $P(\theta)$ at $T=210$ K for many observation times in the ballistic and cage regimes in Fig. 7. For very short times ($\Delta t<50$ fs), we find that $P(\theta)$ is uniformly distributed and we observe no correlation between the maximum displacement vectors of neighboring mobiles molecules. This can be understood because at short time scales the MM-clusters and clusters formed by randomly selected molecules are nearly indistinguishable. Differences from the random case start to emerge at $\Delta t\approx 60$ fs and reach their maximum at $\Delta t=0.26$ ps, i.e., at the beginning of the cage regime when molecules reach the boundaries of their cages. These small Δt differences are due to correlations in vibrational motions due to hydrogen bonding. We observe that $P(\theta)$ increases for $\theta\approx 0°$ indicating that neighboring mobile molecules move preferentially parallel to each other. During the cage regime (until $\Delta t\lesssim t^*=65.54$ ps), $P(\theta)$ still has a maximum at small angles but it evolves to a uniform distribution as Δt increases.

Having established that molecules preferentially displace parallel to each other, we next investigate whether the magnitude of the displacements of the molecules are similar. In Fig. 8 we show the probability density function $P(\Delta r_{ij})$, where Δr_{ij} is the change in the distance between any two

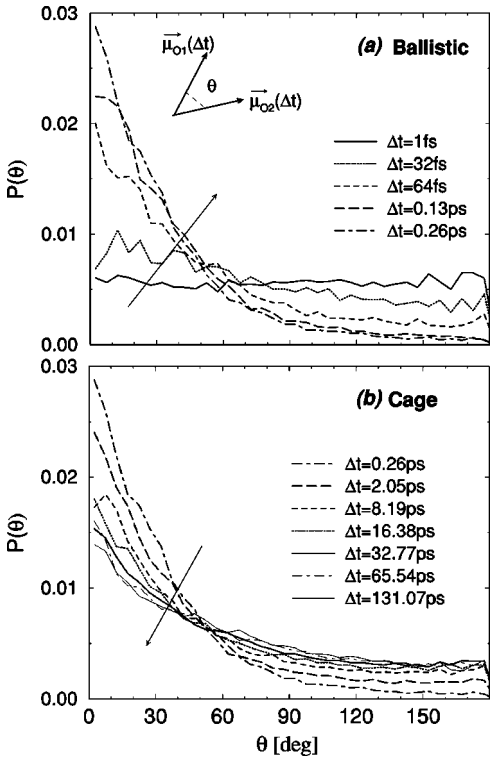

FIG. 7. Probability density function $P(\theta)$ for the angle θ between the maximum displacement vectors $\vec{\mu}_{O1}(\Delta t)$ and $\vec{\mu}_{O2}(\Delta t)$ of two neighbor oxygen atoms belonging to the same MM-cluster. We show $P(\theta)$ at $T=210$ K for different values of the observation time Δt corresponding to the (a) ballistic and (b) cage regimes. For short Δt, $P(\theta)$ is uniform as expected for clusters formed by randomly chosen molecules. The maximum peak at 0° is reached for $t=0.26$ ps, just at the end of the ballistic regime and the beginning of the cage regime. During the cage regime, $P(\theta)$ decreases at $\theta=0°$ evolving toward a uniform distribution.

nearest-neighbor mobile molecules i,j in the interval t_0 and t_0+t^* at $T=210$ K. Specifically,

$$\Delta r_{ij} = ||\vec{r}_i(t_0+t^*) - \vec{r}_j(t_0+t^*)| - |\vec{r}_i(t_0) - \vec{r}_j(t_0)||. \quad (27)$$

If mobile molecule i and j move in a stringlike manner, then the distance between them should not significantly change, i.e., we should find $\Delta r_{ij}=0$. Figure 8 shows that this is the dominant case, i.e., $P(\Delta r_{ij})$ has a sharp peak at $\Delta r_{ij}=0$. This result is consistent with the peak found in $P(\theta)$ at $\theta=0°$ for $\Delta t=t^*\approx 65$ ps at $T=210$ K. Note that when calculating the $P(\Delta r_{ij})$ for all mobile molecules, i.e., not only nearest-neighbors, the sharp peak at $\Delta r_{ij}=0$ is not present; this reflects the ramified structure of the cluster as a whole. The fact that $P(\Delta r_{ij})\neq 0$ for $\Delta r_{ij}>0.05$ nm means that in many cases, molecules also move away from each other, as we observe in Fig. 7, where $P(\theta=180°)\neq 0$.

Finally, we determine whether the displacements of neighboring oxygen atoms are collinear with the direction connecting the two oxygens by studying the angles α_{O1} and α_{O2}. Figure 9(a) shows schematically two oxygen atoms O_1 and O_2 belonging to nearest-neighbor mobile molecules. α_{O1} and α_{O2} are the angles between the direction connecting oxygens O_1 and O_2 and the maximum displacement vectors of each oxygen $\vec{\mu}_{O1}(\Delta t=t^*)$ and $\vec{\mu}_{O2}(\Delta t=t^*)$, during an observation time $\Delta t=t^*$. In a hydrogen bond a molecule shares one of its hydrogen atoms with one of its neighbors [63]. In this way, one molecule "donates" a hydrogen atom and the other molecule "accepts" it [64]. In Fig. 9(a), O_1 is the acceptor oxygen atom while O_2 is the donor oxygen. We also define in Fig. 9(a) the angle α_{OH} between the shared hydrogen atom

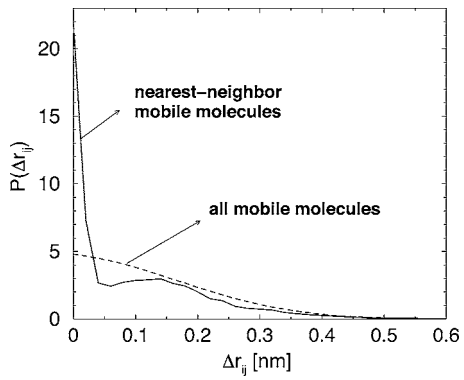

FIG. 8. Probability density function for the change in the distance Δr_{ij} between two nearest-neighbor mobile molecules i,j in the interval t_0 and t_0+t^*. More precisely, $\Delta r_{ij}\equiv||\vec{r}_i(t_0+t^*)-\vec{r}_j(t_0+t^*)|-|\vec{r}_i(t_0)-\vec{r}_j(t_0)||$. The sharp peak at $\Delta r_{ij}=0$ implies that mobile molecules, after a time t^*, mainly conserve their relative distance. When calculating $P(\Delta r_{ij})$ for all mobile molecules, i.e., not only nearest-neighbors, the sharp peak at $\Delta r_{ij}=0$ is not present, reflecting the ramified structure of the cluster as a whole.

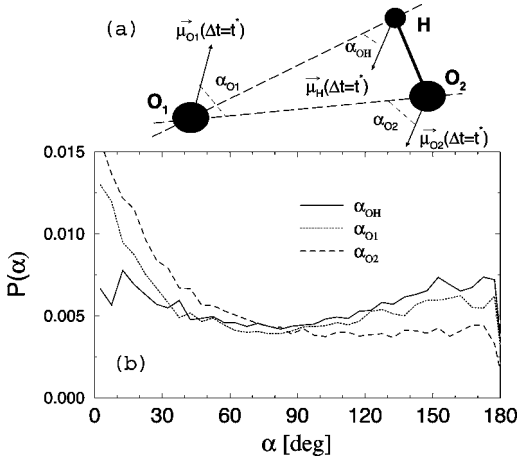

FIG. 9. (a) Schematic illustration showing the angles α_{O1}, α_{O2}, and α_{OH} defined for pairs of neighbor molecules in a MM-cluster. O_2 is the oxygen atom of the donor molecule which shares one of its hydrogen atoms with the acceptor oxygen atom O_1. $\vec{\mu}_{O1}(\Delta t=t^*)$, $\vec{\mu}_{O2}(\Delta t=t^*)$, and $\vec{\mu}_{H}(\Delta t=t^*)$ are the maximum displacement vectors during an observation time $\Delta t=t^*$ corresponding to oxygens O_1, O_2, and the shared hydrogen H. Here, α_{O1} and α_{O2} are the angles between the O_1-O_2 direction and the vectors $\vec{\mu}_{O1}(\Delta t=t^*)$ and $\vec{\mu}_{O2}(\Delta t=t^*)$, respectively. α_{OH} is the angle between $\vec{\mu}_{H}(\Delta t=t^*)$ and the O_1-H direction. (b) Probability density function at $T=210$ K for the angles α_{O1}, α_{O2}, and α_{OH} defined schematically in (a). The α_{O1} and α_{O2} distributions have sharp peaks at $\alpha=0°$ suggesting that molecules move preferentially toward a neighboring molecule.

maximum displacement vector and the direction connecting the acceptor oxygen atom O_1 and the hydrogen atom. Figure 9(b) shows the probability density functions for each of these angles at $T=210$ K. The α_{01} and α_{02} distributions are peaked at 0° suggesting that molecules move preferentially toward a neighboring molecule. However, distributions are nonzero for $\alpha=180°$, meaning that sometimes molecules move apart from each other. Hence molecules predominantly move in a collinear fashion as observed in the LJ and polymer systems [23,31]. We note that the α_{OH} distribution is peaked at 0° and $\approx 180°$ and is approximately symmetric around 90°. This suggests that the H atoms tend to rotate toward or away from the acceptor oxygen atom O_1 with equal probability [65].

VI. RELATION BETWEEN SHD AND TRANSITIONS BETWEEN INHERENT STRUCTURES

It has been suggested that diffusion in cold liquids may be a consequence of a collection of smaller and more subtle types of heterogeneity that would occur when the system moves between consecutive local minima (IS) in the PEL [44–46]. In Ref. [46] we studied the transitions between IS using the SPC/E model and found that molecules with larger displacements in IS transitions form clusters, i.e., IST-clusters. IST-clusters similar to those found in the SPC/E model have been also found in binary mixtures of LJ particles [45]. In this section we study how the IST-clusters [46] relate to the MM-clusters obtained in the equilibrium trajectory studied in Sec. III.

To compare these types of clusters, we follow both the equilibrium MD-trajectory and the corresponding IS-trajectory, i.e., the trajectory obtained by successive energy minimizations of the equilibrium trajectory as a function of time. We again focus on the fraction $\phi=0.07$ of the most mobile molecules. MM-clusters in the equilibrium trajectory are identified as explained in Sec. III. The same definition is used to identify IST-clusters in the IS-trajectory, except that we use the coordinates of the molecules from the IS-trajectory. This definition of the IST-clusters is identical to the definition used in Ref. [46] when Δt is small enough so that there is only one IS-transition between t_0 and $t_0+\Delta t$.

In the following analysis, we show how the MM-clusters in the equilibrium trajectory defined at t_0 with an observation time Δt relate to the IST-clusters in the IS-trajectory defined also at t_0 with the same observation time Δt. Figure 10 shows the mean-square displacement $\langle r^2(\Delta t)\rangle$ of the equilibrium trajectory at $T=210$ K and the average number of molecules $\langle k(\Delta t)\rangle$ which belong both to the MM-clusters and the IST-clusters. We normalize $\langle k(\Delta t)\rangle$ by $N\phi$, so, the equality $\langle k(\Delta t)\rangle/N\phi=1$ implies that MM-clusters and IST-clusters totally overlap. We find a correlation between $\langle k(\Delta t)\rangle/N\phi$ and $\langle r^2(\Delta t)\rangle$. During the ballistic regime $\langle k(\Delta t)\rangle/N\phi<0.1$ and it does not change with Δt. For the case in which the molecules in each subset are independently and randomly chosen, the expected value is

$$\frac{\langle k(\Delta t)\rangle}{N\phi}=\phi=0.07. \tag{28}$$

Thus the identities of the molecules in the MM-clusters and the IST-clusters have virtually no overlap. This result suggests that in this time frame there is little relation between the motions of the molecules in the equilibrium trajectory and the motions of the molecules when the system changes from one IS to another. The overlap between MM-clusters and the IST-clusters is larger during the cage regime, and $\langle k(\Delta t)\rangle/N\phi$ increases as $\log(\Delta t)$. Once the diffusive regime starts, $\langle k(\Delta t)\rangle/N\phi$ evolves very slowly with Δt, approaching its maximum value of 1.

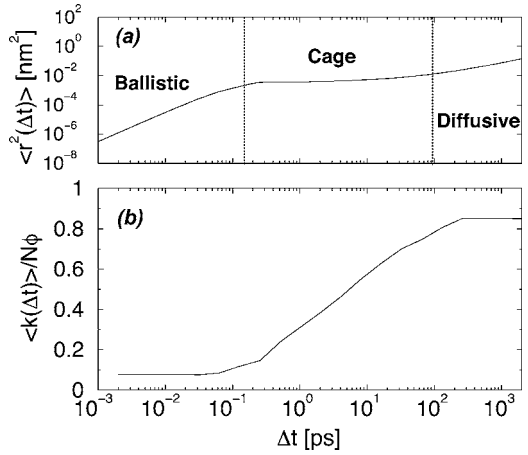

FIG. 10. (a) Mean square displacement at $T=210$ K showing approximately the transition from the ballistic to the cage regime and from the cage to the diffusive regime. (b) Normalized average number of molecules, $\langle k(\Delta t)\rangle/N\phi$, which belong to both the MM-clusters and the IST-clusters found in the IS-trajectory. The normalization factor is $N\phi=216\times 0.07\approx 15$, i.e., the maximum number of mobile molecules for this system. $\langle k(\Delta t)\rangle/N\phi$ shows that both types of clusters are uncorrelated during the ballistic regime, but as Δt increases in the cage regime both types of clusters share more molecules. In the diffusive regime, MM-clusters and the IST-clusters tend to overlap.

In Fig. 11 we show the probability $P(k)$ that k molecules belong to both MM-clusters and IST-clusters as a function of the observation time Δt. We show $P(k)$ (a) during the ballistic regime ($\Delta t \lesssim 0.2$ ps), and (b) during the cage regime (0.2 ps $\lesssim \Delta t \lesssim 100$ ps) and diffusive regime ($\Delta t \gtrsim 100$ ps). The behavior of $P(k)$ for different Δt is consistent with the evolution of $\langle k(\Delta t)\rangle/N\phi$. There is a weak time dependence of $P(k)$ during the ballistic regime with the maximum at $k=1$, while the distribution during the cage regime shifts rapidly to higher values of k. At the beginning of the diffusive regime there is still a weak shift of $P(k)$ to larger values of k.

To better understand our results, we refer to Fig. 12 where we show schematically the basins in the PEL sampled at time t_0 and at time $t_0+\Delta t$. We define $\mathbf{R_{IS}}(t)$ as a $3N$-dimensional vector given by the coordinates of all the oxygen atoms at the IS sampled at time t. We then define the vector $\Delta\mathbf{R_{IS}}(\Delta t)$ pointing from the starting IS at t_0 to the IS sampled at time $t_0+\Delta t$,

$$\Delta\mathbf{R_{IS}}(\Delta t)\equiv\mathbf{R_{IS}}(t_0+\Delta t)-\mathbf{R_{IS}}(t_0). \tag{29}$$

Analogously, we also identify $\mathbf{R}(t)$ as a $3N$-dimensional vector given by the coordinates of all the oxygen atoms at time t, and define

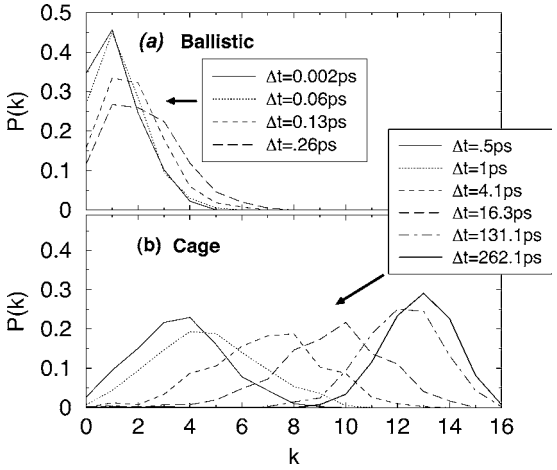

FIG. 11. Probability density function $P(k)$ that k molecules belonging to MM-clusters also belong to IST-clusters for different observation times Δt. In accord with Fig. 10, during the ballistic regime $P(k)$ is centered at $k=1$ but its width increases with Δt. During the cage regime $P(k)$ shifts to larger values of k. We find that during the diffusive regime, $P(k)$ continues to shift slowly to larger values of k and its width decreases.

$$\Delta \mathbf{R}(\Delta t) \equiv \mathbf{R}(t_0 + \Delta t) - \mathbf{R}(t_0). \tag{30}$$

Here $\Delta \mathbf{R}(\Delta t)$ is a $3N$-dimensional vector pointing from the starting configuration at time t_0 to the configuration at time $t_0+\Delta t$; this definition implies mathematically that $\langle \Delta \mathbf{R}^2(\Delta t)\rangle = N\langle r^2(\Delta t)\rangle$. The vector $\mathbf{d}(t)$ in Fig. 12 points from the IS sampled at t to the configuration of the system at t, i.e.,

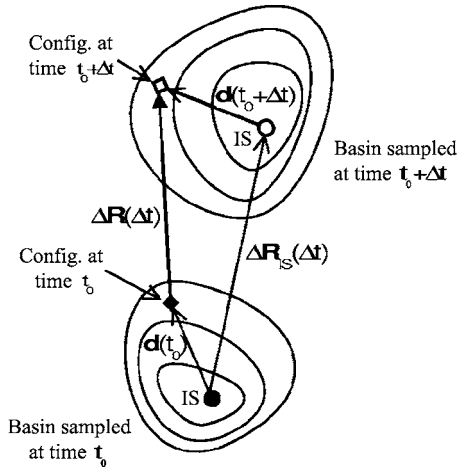

FIG. 12. Scheme showing one basin in the PEL sampled at time t_0 and another basin sampled at time $t_0+\Delta t$. $\Delta \mathbf{R}_{\mathbf{IS}}(\Delta t)$ is the vector pointing from the starting IS sampled at t_0 to the IS sampled at time $t_0+\Delta t$ and $\Delta \mathbf{R}(\Delta t)$ is the vector pointing from the starting configuration of the system at t_0 to the configurations at time $t_0+\Delta t$. $\mathbf{d}(t)$ is the vector pointing from the IS sampled at time t to the configuration of the system at the same time. For $\Delta t \approx 0$, $|\mathbf{d}(t_0+\Delta t)| \approx |\Delta \mathbf{R}(\Delta t)|$, $|\Delta \mathbf{R}_{\mathbf{IS}}(\Delta t)|$. For long Δt, $|\mathbf{d}(t_0+\Delta t)|$ and $|\mathbf{d}(t_0)|$ are much smaller than $|\Delta \mathbf{R}(\Delta t)|$ or $|\Delta \mathbf{R}_{\mathbf{IS}}(\Delta t)|$, therefore $\Delta \mathbf{R}(\Delta t) \approx \Delta \mathbf{R}_{\mathbf{IS}}(\Delta t)$. The condition $\Delta \mathbf{R}(\Delta t) \approx \Delta \mathbf{R}_{\mathbf{IS}}(\Delta t)$ satisfied for long Δt implies that MM-clusters and IST-clusters overlap.

$$\mathbf{d}(t) \equiv \mathbf{R}(t) - \mathbf{R}_{\mathbf{IS}}(t). \tag{31}$$

We note that MM-clusters are defined from the displacement of the molecules in the real trajectory, i.e., from the components of $\Delta \mathbf{R}(\Delta t)$. Instead, IST-clusters are defined from the displacement of the molecules in the IS-trajectory, i.e., from the components of $\Delta \mathbf{R}_{\mathbf{IS}}(\Delta t)$. Therefore, when these two vectors are approximately the same, $|\mathbf{d}(t_0+\Delta t)|$, $|\mathbf{d}(t_0)| \ll |\Delta \mathbf{R}_{\mathbf{IS}}(\Delta t)|$, we will find that MM-clusters and IST-clusters overlap.

At $T=210\ \mathrm{K} > T_{MCT}$, $\Delta \mathbf{R}^2(\Delta t)$ grows continuously with time while $\mathbf{d}^2(\Delta t)$ is bounded. We find $\mathbf{d}^2(t) \sim 0.5\ \mathrm{nm}^2$ meaning that the configurations are always close to their corresponding IS—i.e., the root-mean-square distance between the positions of an oxygen atom in a given configuration and in the corresponding IS is $\sqrt{\mathbf{d}^2(t)/N} \sim 0.05$ nm. For very short times, the two basins in Fig. 12 are neighboring and $\Delta \mathbf{R}^2(\Delta t) \lesssim \mathbf{d}^2(t_0+\Delta t)$, e.g., we find that for $\Delta t = 0.1$ ps,

$$\frac{\Delta \mathbf{R}^2(\Delta t)}{\mathbf{d}^2(t_0 + \Delta t)} \approx 0.43. \tag{32}$$

Therefore molecules belonging to the MM-clusters and the IST-clusters are expected to be different. $P(k)$ confirms this expectation, as shown in Fig. 11(a). During the cage regime and at later times, $\Delta \mathbf{R}^2(\Delta t) > \mathbf{d}(\Delta t)^2$ and therefore, as time goes on, $\Delta \mathbf{R}(\Delta t)$ approaches $\Delta \mathbf{R}_{\mathbf{IS}}(\Delta t)$. In other words, more and more molecules belonging to the MM-clusters will also belong to the IST-clusters in agreement with Fig. 11(b). Finally, in the diffusive regime, $\Delta \mathbf{R}(\Delta t) \approx \Delta \mathbf{R}_{\mathbf{IS}}(\Delta t)$ and MM-clusters overlap with IST-clusters.

Next, we discuss briefly how the MM-clusters and the IST-clusters are related with the topography of the PEL. Stillinger [44] suggested that the PEL is very rough and many small contiguous basins may be grouped together to form wider "megabasins." The elementary transition processes (identified with the β-relaxation [44]) that connect the small contiguous basins require only local rearrangements of a small number of particles. The escape from one "megabasin" to another requires a lengthy directed sequence of elementary transitions [66,67]. In the context of the topography of the PEL, the IST-clusters identified in [46], i.e., in the transitions between *consecutive* IS, should be identified with the elementary processes suggested in [44]. Instead, the MM-clusters (defined with $\Delta t = t^*$) may be related to transitions between megabasins [66,67].

VII. SUMMARY

We have presented a detailed analysis of the MM-clusters characterizing the spatially heterogeneous dynamics in water. Similar to other simulations of atomic and polymer systems, clusters are largest on the time scale of the onset of diffusive motion and their size increases nonlinearly with T upon cooling. The probability density function for the cluster size follows a power law with exponent ≈ 2, as also found in atomic systems. The correlation length of the MM-clusters corresponds to a typical spatial dimension of the order of 1 nm, comparable to the length scale found in simulations of LJ

systems [21]. However, further simulations at lower temperature are needed to better compare with estimates obtained for the length scale of SHD in experiments close to the glass transition temperature [54]. We do not find a power law relating the size of the MM-clusters and the correlation length (expected from percolation theory), as is the case for simulations of a polymer melt [30]. This is most likely a result of the fact that MM-clusters are branched, and that there are mainly small MM-clusters with two or three molecules. As a consequence, the size of the MM-clusters has an exponential dependence on the correlation length which will only approach a power-law dependence for MM-clusters larger than those obtained in this study.

Motivated by the AG theory, we also study the MM-cluster properties as a function of the configurational entropy. We find evidence suggesting that the MM-clusters obey the functional form relating entropy and size proposed by AG for the cooperatively rearranging regions. This result, combined with the AG predictions, gives an estimation for the cluster size at T_g of 2 to 3 molecules which is in agreement with experimental clusters size measurements in OTP [36].

Within the MM-clusters, we found that a molecule mainly follows its neighbor molecule, as is the case of LJ and polymeric liquids. This result supports the hypothesis [23] that stringlike motion may be a generic mechanism of both simple atomic liquids and complex molecular liquids.

In the last part of this work we considered the relation between the MM-clusters formed in the equilibrium trajectory and the IST-clusters formed in the IS trajectory. We find that both types of clusters are different for short time scales, meaning that experiments detecting SHD in short time scales ($\lesssim$0.2 ps) cannot give information on clusters found in IS transitions. However, MM-clusters and IST-clusters overlap on the longer time scales of diffusive motion, where the system is changing PEL megabasins [44], so, MM-clusters can be related to clusters between IS in different megabasins of the PEL.

ACKNOWLEDGMENTS

We thank S.C. Glotzer, M. Mazza, and especially A. Coniglio for enlightening discussions on the connection between percolation theory and the mobile clusters studied in this work. This work was supported by NSF Chemistry Grants CHE0096892 and CHE0404673.

[1] S. C. Glotzer, J. Non-Cryst. Solids **274**, 342 (2000).
[2] M. D. Ediger, Annu. Rev. Phys. Chem. **51**, 99 (2000).
[3] R. Richert, J. Phys.: Condens. Matter **14**, R703 (2002).
[4] J. P. Garrahan and D. Chandler, Phys. Rev. Lett. **89**, 035704 (2002).
[5] J. P. Garrahan and D. Chandler, Proc. Natl. Acad. Sci. U.S.A. **100**, 9710 (2003).
[6] Facilitated models were introduced in G. H. Fredrickson and H. C. Andersen, Phys. Rev. Lett. **53**, 1244 (1984).
[7] An analysis of dynamical heterogeneity related to that presented in [4,5] is discussed in S. Butler and P. Harrowell, J. Chem. Phys. **95**, 4454 (1991).
[8] The idea of critical scaling in glasses is discussed in R. Yamamoto and A. Onuki, Phys. Rev. E **58**, 3515 (1998).
[9] G. Adam and J. H. Gibbs, J. Chem. Phys. **43**, 139 (1965).
[10] M. Vogel and S. C. Glotzer, Phys. Rev. Lett. **92**, 255901 (2004).
[11] In fact, according to Adam and Gibbs, it was E. Jenckel [Z. Phys. Chem. Abt. A **184**, 309 (1939)] who first discussed the temperature dependence of the size of the CRR.
[12] For a clear description of the physical basis of AG theory, see P. G. Debenedetti, *Metastable Liquids* (Princeton University Press, Princeton, 1996).
[13] It should be noted that the GC approach is at odds with the AG theory since thermodynamics is completely decoupled from dynamics in facilitated models.
[14] R. Richert and C. A. Angell, J. Chem. Phys. **108**, 9016 (1998).
[15] R. Casalini, S. Capaccioli, M. Lucchesi, P. A. Rolla, and S. Corezzi, Phys. Rev. E **63**, 031207 (2001); R. Casalini *et al.*, *ibid.* **64**, 041504 (2001).
[16] S. Sastry, Nature (London) **409**, 164 (2001); S. Mossa, E. La Nave, H. E. Stanley, C. Donati, F. Sciortino, and P. Tartaglia, Phys. Rev. E **65**, 041205 (2002).
[17] F. H. Stillinger and T. A. Weber, J. Phys. Chem. **87**, 2833 (1983); F. Sciortino *et al.*, Phys. Rev. Lett. **83**, 3214 (1999); B. Coluzzi, G. Parisi, and P. Verrocchio *ibid.* **84**, 306 (1999).
[18] A. Scala, F. W. Starr, E. La Nave, F. Sciortino, and H. E. Stanley, Nature (London) **406**, 166 (2000).
[19] F. W. Starr, S. Sastry, E. La Nave, A. Scala, H. E. Stanley, and F. Sciortino, Phys. Rev. E **63**, 041201 (2001); F. W. Starr, C. A. Angell, E. La Nave, S. Sastry, A. Scala, F. Sciortino, and H. E. Stanley, Biophys. Chem. **105**, 573 (2003).
[20] H. Tanaka, Phys. Rev. Lett. **90**, 055701 (2003).
[21] W. Kob, C. Donati, S. J. Plimpton, P. H. Poole, and S. C. Glotzer, Phys. Rev. Lett. **79**, 2827 (1997).
[22] C. Donati, J. F. Douglas, W. Kob, S. J. Plimpton, P. H. Poole, and S. C. Glotzer, Phys. Rev. Lett. **80**, 2338 (1998).
[23] S. C. Glotzer, P. H. Poole, W. Kob, and S. J. Plimpton, Phys. Rev. E **60**, 3107 (1999).
[24] C. Bennemann, J. Baschnagel, and S. C. Glotzer, Nature (London) **399**, 246 (1999).
[25] M. Hurley and P. Harrowell, Phys. Rev. E **52**, 1694 (1995).
[26] B. Doliwa and A. Heuer, Phys. Rev. Lett. **80**, 4915 (1998).
[27] A. I. Mel'cuk, R. A. Ramos, H. Gould, W. Klein, and R. D. Mountain, Phys. Rev. Lett. **75**, 2522 (1995).
[28] N. Lačević, F. W. Starr, T. B. Schrøder, V. N. Novikov, and S. C. Glotzer, Phys. Rev. E **66**, 030101 (2002).
[29] N. Lačević, T. B. Schrøder, F. W. Starr, V. N. Novikov, and S. C. Glotzer, J. Chem. Phys. **119**, 7372 (2003).
[30] Y. Gebremichael, T. B. Schrøder, F. W. Starr, and S. C. Glotzer, Phys. Rev. E **64**, 051503 (2001).
[31] M. Aichele, Y. Gebremichael, F. W. Starr, J. Baschnagel, and S. C. Glotzer, J. Chem. Phys. **119**, 5290 (2003).
[32] Y. Gebremichael, M. Vogel, and S. C. Glotzer, J. Chem. Phys.

120, 4415 (2004).
[33] W. K. Kegel and A. van Blaaderen, Science **287**, 290 (2000).
[34] A. Heuer, M. Wilhelm, H. Zimmermann, and H. W. Spiess, Phys. Rev. Lett. **75**, 2851 (1995).
[35] K. Schmidt-Rohr and H. W. Spiess, Phys. Rev. Lett. **66**, 3020 (1991); J. Liesen, K. Schmidt-Rohr, and H. W. Spiess, J. Non-Cryst. Solids **172**, 737 (1994); R. Böhmer *et al.*, Europhys. Lett. **36**, 55 (1996); B. Schiener *et al.*, Science **274**, 752 (1996).
[36] M. T. Cicerone, F. R. Blackburn, and M. D. Ediger, J. Chem. Phys. **102**, 471 (1995).
[37] F. Fujara, B. Geil, H. Sillescu, and G. Fleischer, Z. Phys. B: Condens. Matter **88**, 195 (1992); H. Sillescu, J. Non-Cryst. Solids **243**, 81 (1999).
[38] E. R. Weeks, J. C. Crocker, A. C. Levitt, A. Schofield, and D. A. Weitz, Science **287**, 627 (2000).
[39] N. Giovambattista, S. V. Buldyrev, F. W. Starr, and H. E. Stanley, Phys. Rev. Lett. **90**, 085506 (2003).
[40] N. Giovambattista, M. G. Mazza, S. V. Buldyrev, F. W. Starr, and H. E. Stanley, J. Phys. Chem. B **108**, 6655 (2004).
[41] H. J. Berendsen, J. R. Grigera, and T. P. Straatsma, J. Phys. Chem. **91**, 6269 (1987).
[42] M. Goldstein, J. Chem. Phys. **51**, 3728 (1969).
[43] F. H. Stillinger and T. A. Weber, Phys. Rev. A **28**, 2408 (1983).
[44] F. H. Stillinger, Science **267**, 1935 (1995); P. G. Debenedetti and F. H. Stillinger, Nature (London) **410**, 259 (2001).
[45] T. B. Schrøder, S. Sastry, J. C. Dyre, and S. C. Glotzer, J. Chem. Phys. **112**, 9834 (2000).
[46] N. Giovambattista, F. W. Starr, F. Sciortino, S. V. Buldyrev, and H. E. Stanley, Phys. Rev. E **65**, 041502 (2002).
[47] F. W. Starr, S. Harrington, F. Sciortino, and H. E. Stanley, Phys. Rev. Lett. **82**, 3629 (1999); F. W. Starr, F. Sciortino, and H. E. Stanley, Phys. Rev. E **60**, 6757 (1999).
[48] W. Götze, J. Phys.: Condens. Matter **11**, A1 (1999); W. Götze, in *Liquids, Freezing and Glass Transition*, edited by J. P. Hansen, D. Levesque, and J. Zinn-Justin (North-Holland, Amsterdam, 1991).
[49] J. P. Hansen and I. R. McDonald, *Theory of Simple Liquids* (Academic Press, London, 1986).
[50] F. Sciortino, P. Gallo, P. Tartaglia, and S.-H. Chen, Phys. Rev. E **54**, 6331 (1996).
[51] Note that the first neighbor oxygen-oxygen distance between molecules for SPC/E is $\approx$0.28 nm.
[52] Alternatively, we also consider using a separation of 0.35 nm, the distance criterion commonly used by hydrogen bond definitions [F. Sciortino and S. L. Fornili, J. Chem. Phys. **90**, 2786 (1989)]. Preliminary calculations indicate this alternative choice does not qualitatively affect our results.
[53] D. Stauffer and A. Aharony, *Introduction to Percolation Theory* (Taylor and Francis, London, 1998).
[54] M. T. Cicerone and M. D. Ediger, J. Chem. Phys. **103**, 5684 (1995).
[55] *Fractals and Disordered Systems*, edited by A. Bunde and S. Havlin (Springer-Verlag, Berlin, 1996).
[56] J.-P. Bouchaud, cond-mat/0211196.
[57] H. E. Castillo, C. Chamon, L. F. Cugliandolo, J. L. Iguain, and M. P. Kennett, Phys. Rev. B **68**, 134442 (2003).
[58] In computer simulations S_{conf} is usually calculated by the multiplicity of potential energy minima, or by the difference $S_{\mathrm{conf}}(T,V) \equiv S(T,V) - S_{\mathrm{vib}}(T,V)$, where $S(T,V)$ and $S_{\mathrm{vib}}(T,V)$ are the total and vibrational entropy of the system at (T,V), respectively. To calculate S, first $S(T_0,V_0)$ is calculated at a reference point (T_0,V_0) and then $S(T,V)$ is calculated by thermodynamic integration using the relationship $dS = dE/T + PdV/dT$. $S_{\mathrm{vib}}(T,V)$ is the entropic contribution due to the vibrational motion of the system in a basin of the PEL. It is usually estimated by $S_{\mathrm{vib}}(T,V) = S_{\mathrm{harm}}(T,V) + S_{\mathrm{anharm}}(T,V)$, where $S_{\mathrm{harm}}(T,V)$ is the entropy of a $6N$-dimensional harmonic oscillator (in the case of water, which has six degrees of freedom for each molecule) and $S_{\mathrm{anharm}}(T,V)$ is a correction term for possible anharmonic oscillations of the system in the basins. $S_{\mathrm{anharm}}(T,V)$ is obtained by heating configurations corresponding to IS sampled at (T,V) from $T=0$ K up to $T=200$ K and measuring the total energy of the system as a function of T. For the SPC/E model [14], it is found that $S_{\mathrm{anharm}}(T,V) = AT + BT^2$ approximates the behavior of the anharmonic contribution, where A and B are adjustable constants determined by the behavior of the energy on heating.
[59] C. A. Angell, K. L. Ngai, G. B. McKenna, P. F. McMillan, and S. W. Martin, J. Appl. Phys. **88**, 3113 (2000).
[60] E. Donth, J. Non-Cryst. Solids **53**, 325 (1982).
[61] Y. Gebremichael, M. Vogel, M. Bergroth, F. W. Starr, and S. C. Glotzer (unpublished).
[62] M. Vogel and S. C. Glotzer, Phys. Rev. E **70**, 061504 (2004).
[63] We calculate the distance between each hydrogen atom of one molecule to the oxygen of the other molecule. The shortest of these four distances defines the hydrogen atom shared by the two molecules.
[64] F. W. Starr, J. K. Nielsen, and H. E. Stanley, Phys. Rev. Lett. **82**, 2294 (1999); Phys. Rev. E **62**, 579 (2000).
[65] M. Mazza, N. Giovambattista, F. W. Starr, and H. E. Stanley (unpublished).
[66] B. Doliwa and A. Heuer, Phys. Rev. E **67**, 030501 (2003); **67**, 031506 (2003); R. A. Denny, D. R. Reichman, and J.-P. Bouchaud, Phys. Rev. Lett. **90**, 025503 (2003).
[67] M. Vogel, B. Doliwa, A. Heuer, and S. C. Glotzer, J. Chem. Phys. **120**, 4404 (2004).